Separation Science and Technology
Publication details, including instructions for authors and subscription information:
http://www.informaworld.com/smpp/title~content=t713708471

Overview of Fouling Phenomena and Modeling Approaches for Membrane Bioreactors

Chia-Chi Ho[a]; Andrew L. Zydney[b]
[a] Department of Chemical and Materials Engineering, University of Cincinnati, Cincinnati, OH [b] Department of Chemical Engineering, The Pennsylvania State University, University Park, PA

To cite this Article Ho, Chia-Chi and Zydney, Andrew L.(2006) 'Overview of Fouling Phenomena and Modeling Approaches for Membrane Bioreactors', Separation Science and Technology, 41: 7, 1231 — 1251
To link to this Article: DOI: 10.1080/01496390600632297
URL: http://dx.doi.org/10.1080/01496390600632297

Separation Science and Technology, 41: 1231–1251, 2006

ISSN 0149-6395 print/1520-5754 online
DOI: 10.1080/01496390600632297

Overview of Fouling Phenomena and Modeling Approaches for Membrane Bioreactors

Chia-Chi Ho
Department of Chemical and Materials Engineering,
University of Cincinnati, Cincinnati, OH

Andrew L. Zydney
Department of Chemical Engineering,
The Pennsylvania State University, University Park, PA

Abstract: Membrane bioreactors are used extensively for the treatment of municipal and industrial wastewaters. Membrane fouling remains a critical issue in the design and operation of these systems. The complex nature of the feed, the high solids concentration, and the limited options available for pretreatment and cleaning all serve to exacerbate the problem of membrane fouling. This manuscript provides an overview of the key fouling phenomena involved in membrane bioreactors, with a particular emphasis on the nature of the fouling components and the different modeling approaches used to describe the flux decline and to identify the underlying fouling mechanisms.

Keywords: Membrane bioreactors, membrane fouling, modeling approaches, flux decline

Received 10 January 2006, Accepted 23 January 2006

Submitted to Separation Science and Technology, Special Issue on Membrane Fouling and Fouling Control in Membrane Bioreactor and Related Biological Process.

Address correspondence to Andrew L. Zydney, Department of Chemical Engineering, The Pennsylvania State University, University Park, PA 16802, USA. Tel.: 814-863-7113; Fax: 814-865-7846; E-mail: zydney@engr.psu.edu

INTRODUCTION

Although much of the early interest in membrane bioreactors was focused on the production of high value biological products (1) or the development of bioartificial organs (2), the most extensive commercial applications of this technology have been in the area of wastewater treatment (3). This includes very large scale applications of the Kubota, ZenoGem, ZeeWeed, Orelis, Biosuf, and Aduf membrane bioreactor systems for municipal wastewater treatment around the world, each with capacities in excess of $1000\,m^3/day$ (3, 4). Membrane bioreactors have also been installed for water recycling in buildings (5), industrial wastewater treatment (6), and landfill leachate treatment (7), and there is growing interest in a variety of agricultural waste treatment appplications (4).

Biological systems, typically employing activated sludge, have been used for wastewater treatment for over a century. Biomass is typically separated from the treated water in a settler/clarifier. Microfiltration and ultrafiltration are sometimes used for tertiary water treatment, providing a highly purified effluent that is able to meet more stringent discharge requirements. Microfiltration membranes, with pore sizes of about 0.08 to 4 μm, provide nearly complete removal of bacteria, significantly reducing the level of chlorination needed for disinfection, thereby minimizing the formation of hazardous disinfection by-products. Tighter pore size ultrafiltration membranes (pore sizes ranging from 0.01 to 0.08 μm) retain viruses and much of the colloidal material, while also reducing the level of natural organic matter in the final treated water.

There are several additional advantages to integrating the membrane unit directly into the biological wastewater treatment process in the form of a membrane bioreactor (MBR). First, the membrane provides the desired biomass separation, eliminating the need for a gravity settler, which is often a major challenge in the design and operation of conventional activated sludge systems. The retention of biomass within the bioreactor provides better control of the microbial population, facilitating the development of many slow-growing microorganisms required for nitrification and the degradation of more complex organics (8). The membrane can also retain many extracellular enzymes and soluble oxidants, creating a more active biological environment for wastewater treatment (9). In addition, the activated sludge can be maintained at much higher biomass concentrations, reducing the total volume of the system and the resulting plant footprint. Mixed liquor concentrations of 25,000 mg/L are common in municipal MBR systems compared to less than 5,000 mg/L in conventional (non-membrane) processes, with the lower levels in conventional systems needed to avoid problems in the gravity settler. Even higher biomass concentrations (up to 80,000 mg/L) can be achieved in some industrial processes employing MBR systems (2). The use of very high biomass concentrations can reduce the cost associated with sludge disposal by as much as a factor of three (10). Membrane

bioreactors are also better able to handle fluctuations in nutrient levels in the wastewater (4).

Membrane bioreactors are operated using one of two basic process configurations: the submerged (or integrated) MBR, in which the membrane module is placed directly in the activated sludge, and the external (or recirculated) MBR, both of which are shown schematically in Fig. 1. The mixed liquor in an external MBR is recirculated through the membrane module by a pump, which provides both high crossflow velocities and relatively high transmembrane pressures (typically 100–500 kPa). A variety of membranes can be used, including tubular, plate-and-frame, rotary disk, and hollow fiber. For the hollow fiber modules, the feed can flow either internally or externally to the hollow fibers, with the membrane skin (the tighter pore size region) facing the feed.

In contrast to the external membrane bioreactor, the filtrate flow in a submerged MBR is driven by the hydraulic head associated with the placement of the membrane module within the liquid, often enhanced by the addition of a small vacuum on the permeate side of the module. Typical transmembrane pressure drops are only 10–80 kPa compared to up to 500 kPa in an external module. An air diffuser is placed directly beneath the module to provide scouring/cleaning of the membrane surface, reducing membrane fouling while simultaneously providing the necessary aeration for the biological treatment. Asymmetric hollow fiber membranes are most commonly employed, with the tight (skin) layer on the external surface of the fiber (facing the feed). Submerged MBR systems appear to be the more economical configuration (10) due to the elimination of the recycle pump and the improved membrane performance associated with the use of lower transmembrane pressures and the scouring of the membrane surface by the air bubbles.

One of the critical issues in the design and operation of any membrane bioreactor is membrane fouling, typically characterized by an irreversible decline in the filtrate flux over time due to interactions with various components in the feedstream. The complex nature of the feed, coupled with the

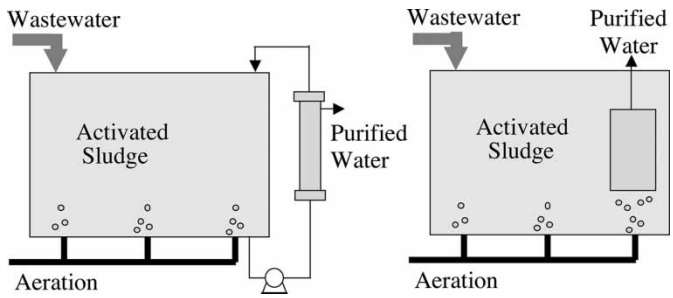

Figure 1. Schematic diagram of external (left panel) and submerged (right panel) membrane bioreactors.

very high solids concentration, tends to exacerbate the problem of membrane fouling. Pretreatment of the feed, which is used extensively in conventional membrane systems, is impractical for membrane bioreactors since the biomass must be effectively retained within the bioreactor. In addition, chemical cleaning of submerged membrane bioreactors is severely limited since most cleaning agents would have an adverse effect on the microorganisms in the activated sludge.

This manuscript provides an overview of the key fouling phenomena in membrane bioreactor systems, with a particular emphasis on the nature of the fouling components and the different modeling approaches that have been used to provide insights into the underlying fouling mechanisms and the magnitude of the flux decline.

FOULING COMPONENTS

Activated sludge is a complex and highly variable suspension containing an array of microorganisms, components present in the feed wastewater, and metabolites and other biomolecules produced within the bioreactor. Many of these components can contribute to membrane fouling, both by adsorption on and within the membrane pores and by deposition (cake layer formation) on the external surface of the membrane.

Biological treatment systems rely upon a range of micro-organisms to effect the desired conversion of soluble and particulate organic compounds. Bacteria are the dominant species, although higher order micro-organisms like protozoa and rotifers play an important role in consuming particulate matter and scavenging bacteria (3). Even larger organisms, e.g., nematode worms and insect larvae, can contribute to the overall biological activity. Ghyoot and Verstaete (11) reported higher concentrations of protozoa, particularly flagellates and free ciliates, in a submerged MBR compared to a conventional activated sludge, although this appears to depend upon the specific operating conditions, mass transfer characteristics, and wastewater properties. Most of the micro-organisms exist in large flocs or aggregates, resulting in synergistic microconsortia that facilitate the degradation of organic materials.

Extracellular polymeric substances (EPS) include a wide variety of proteins, polysaccharides, humic substances, and nucleic acids (12). EPS can be generated by cell lysis, active excretion by microorganisms, spontaneous liberation of integral cellular components from the outer membrane of gram-negative bacteria (blebbing), and hydrolysis of natural organic matter present in the feedwater (12). EPS are the primary structural element in biofilms and bacterial flocs, providing the mechanical stability for these structures while facilitating adherence of the biofilm to surfaces. Polysaccharides are generally the dominant EPS in biofilms, although Dignac et al. (13) identified proteins as the dominant species in bacterial flocs formed in an activated sludge. Wisniewski and Grasmick (14) have shown that floc size

distribution can have a significant effect on membrane fouling, with smaller flocs typically leading to a greater degree of fouling.

Extracellular enzymes produced by micro-organisms can play a critical role in the degradation of certain substrates. Membrane bioreactors tend to have much higher concentrations of these soluble enzymes due to their greater retention by the membrane unit, particularly when using smaller pore size ultrafiltration membranes. The overall chemical composition and molecular weight distribution of the EPS depend upon the properties of the wastewater, the distribution of different micro-organisms, and the nutritional status and overall metabolic environment in the membrane bioreactor.

Given the complexity and the large variability in composition of the mixed liquor, it is not surprising that different investigators have identified different species as the critical component involved in membrane fouling. For example, Wisniewski and Grasmick (14) concluded that the soluble fraction of a biological suspension contributed more than 50% of the fouling, with the colloidal and particulate material each providing about 25% of the observed increase in resistance. In contrast, Defrance et al. (15) attributed only 5% of the fouling to the soluble material, with more than 60% of the flux decline arising from particulates. These differences likely arise from differences in the physicochemical properties of the biomass as well as differences in the operating conditions and properties of the membrane bioreactor.

Despite these contradictory results, there is clear evidence that the extracellular polymeric substances play a critical role in the fouling of membrane bioreactors. Chang and Lee (16) showed that an activated sludge having low concentrations of EPS, in this case generated using a synthetic wastewater containing nitrogen-deficient substrates, had significantly higher filtrate flux and less fouling than the control. Similarly, Nagaoka et al. (17) showed that EPS accumulation on the membrane was the primary factor controlling fouling in a small-scale submerged membrane bioreactor. Lesjean et al. (18) compared the behavior of two 2000 L pilot plant systems using an external MBR operated in parallel on the same feedstock but with different denitrification schemes. The fouling rate in the two MBR systems varied nearly linearly with the polysaccharide concentration (glucose equivalents), with no apparent correlation to the chemical oxygen demand, the protein concentration, or the mixed liquor suspended solids. Similar results were reported by Rosenberger et al. (19) based on an analysis of fouling data from several European MBR installations. The filtration index was well correlated with the polysaccharide concentration for data obtained by varying the carbon substrate and for results from different landfill leachate plants.

CLASSICAL FOULING MODELS

Although fouling in membrane bioreactors can be an extremely complex phenomenon, the most common approach for analyzing flux decline data

and identifying the fouling mechanism is to use one of the classical fouling models: standard pore blockage, intermediate pore blockage, pore constriction, and cake filtration (20, 21). Each of these models is based on a generalized form of Darcy's law, with the filtrate flow rate (Q) expressed as:

$$Q = \frac{\Delta P - \sigma_0 \Delta \pi}{\mu(R_m + R_P)} A \tag{1}$$

where μ is the solution viscosity, ΔP is the transmembrane pressure, R_m is the resistance of the clean membrane, R_P is the resistance of the additional deposit or cake that forms on the external surface of the membrane, A is the area available for filtration, and σ_0 and $\Delta\pi$ are the osmotic reflection coefficient and the osmotic pressure difference across the membrane, respectively. The osmotic reflection coefficient is a measure of the permselectivity of the membrane to the foulant. It varies from one for a fully retentive membrane to zero for a nonretentive membrane. The osmotic pressure term in Equation (1) is neglected in the classical fouling models, although this term can become important for ultrafiltration membranes or for heavily fouled microfiltration membranes where the retention of smaller colloidal solutes becomes significant.

In the complete pore blockage model, the volumetric flow rate declines as the available membrane area (A) decreases. Cake formation is assumed to be negligible, corresponding to $R_P = 0$ in equation (1), and the rate of pore blockage is assumed to be proportional to the convective flow of foulant to the membrane surface:

$$\frac{dA}{dt} = -\alpha_1 Q_{open} C_b \tag{2}$$

where C_b is the bulk foulant concentration and α_1 is a pore blockage parameter which is equal to the membrane pore area blocked per unit mass of foulant convected to the membrane surface. Combination of equations (1) and (2) gives the following expression for the filtrate flow rate as a function of time:

$$\frac{Q}{Q_0} = \exp\left(-\frac{\alpha_1 \Delta P C_b}{\mu R_m} t\right) \tag{3}$$

where Q_0 is the initial filtrate flow rate through the clean membrane.

The intermediate pore blockage model accounts for the possibility that particles land on top of other particles when they deposit on the membrane surface. In this case the rate of pore blockage is assumed to be proportional to the fractional area of the membrane remaining uncovered (A/A_0). The volumetric flow rate thus becomes

$$\frac{Q}{Q_0} = \left(1 + \frac{\alpha_1 \Delta P C_b}{\mu R_m} t\right)^{-1} \tag{4}$$

In the pore constriction model, the membrane is assumed to be composed of a uniform array of parallel cylindrical pores. The particles or aggregates are assumed to deposit uniformly on the pore walls throughout the internal membrane volume, with the rate of change in the pore volume assumed to be proportional to the rate of particle convection to the membrane:

$$\frac{d}{dt}(N\pi r_p^2 \delta_m) = -\alpha_{pore} Q C_b \tag{5}$$

where N is the total number of pores, δ_m is the membrane thickness, and α_{pore} is the volume of foulant deposited in the pore interior per unit mass of foulant filtered through the membrane. The membrane resistance is evaluated as a function of the pore radius (r_p) using the Hagen-Poiseuille equation for laminar flow through a parallel array of cylindrical pores:

$$R_m = \frac{8\delta_m}{N\pi r_p^4} \tag{6}$$

The flow rate is evaluated by combining equations (1), (5) and (6) to give:

$$\frac{Q}{Q_0} = \left(1 + \frac{\alpha_{pore} Q_0 C_b}{\pi r_0^2 \delta_m} t\right)^{-2} \tag{7}$$

where r_0 is the initial pore radius.

In the cake filtration model, a uniform deposit or cake is assumed to form on the upper surface of the membrane, with the rate of increase of the hydraulic resistance of the deposit assumed to be directly proportional to the rate of particle convection to the membrane:

$$\frac{dR_p}{dt} = f' R' J C_b \tag{8}$$

where f' is the fraction of foulant that is convected to the membrane that actually adds to the growing deposit and R' is the specific resistance of the cake layer. Substitution of equation (1) into equation (8) gives upon integration:

$$\frac{Q}{Q_0} = \left(1 + \frac{2f' R' Q_0 C_b}{A_0 R_m} t\right)^{-1/2} \tag{9}$$

Fouling in membrane bioreactors has mostly been analyzed using the cake filtration model (22, 23). A more detailed discussion of the underlying assumptions and mathematical development of these models are provided by Hermia (20) and Zeman and Zydney (24).

Many investigators have used the classical fouling models to try to identify the underlying fouling mechanism by plotting the experimental data using linearized forms of the different models. For the intermediate pore blockage model (equation (4)) this involves plotting $1/Q$ versus t, while for the cake filtration model (equation (9)) the filtrate flow rate data

can be linearized by plotting $1/Q^2$ versus t. Comparable expressions for the other models are provided by Hermia (20) and Zeman and Zydney (24). The underlying fouling mechanism is identified by comparing the linear correlations obtained by plotting the data using the different functional relationships. For example, Yu et al. (25) showed that long time data for the filtration of a synthetic wastewater through a U-shaped hollow fiber membrane in a membrane bioreactor could be linearized using the cake filtration model, suggesting that this is the dominant fouling mechanism at long times.

PORE BLOCKAGE AND CAKE FILTRATION MODEL

Although experimental data for flux decline have often been analyzed using the classical fouling models, many studies have reported a transition in fouling mechanism during the filtration of proteins (26), polysaccharides (27), colloidal iron (28), natural organic matter (29–31), and latex particles (32). Ho and Zydney (33) developed a combined pore blockage and cake filtration model to describe this transition in the fouling behavior. In this model, foulants first deposit on the bare membrane, reducing the area available for unhindered filtration. In contrast to the classical pore blockage model, this initial deposit is assumed to be at least partially permeable to fluid flow, i.e., there is a small finite flow through even the "blocked" pores. As the membrane surface becomes more heavily fouled, the foulant will also begin to deposit directly on the fouling layer, causing an increase in the hydraulic resistance to flow associated with the growing deposit. This is exactly what occurs in the classical cake filtration model, although this cake growth is now assumed to occur simultaneously with the coverage (or blockage) of the remaining open area of the membrane. The filtrate flow rate given by the combined pore blockage and cake filtration model can be expressed as (33):

$$Q = Q_0\left[\exp\left(-\frac{\alpha\Delta PC_b}{\mu R_m}t\right) + \int_0^t \frac{\alpha\Delta PC_b}{\mu(R_m + R_p)}\exp\left(\frac{-\alpha\Delta PC_b}{\mu R_m}t_p\right)dt_p\right] \tag{10}$$

with R_p given as a function of t and t_p by

$$R_p = (R_m + R_{p0})\sqrt{1 + \frac{2f'R'\Delta PC_b}{\mu(R_m + R_{p0})^2}(t - t_p)} - R_m \tag{11}$$

R_{p0} is the resistance of the initial deposit on the membrane and t_p is the time at which the deposit begins to grow. Equation (10) explicitly accounts for the variation in the deposited layer resistance over the surface of the membrane associated with the different time at which each region of the membrane is first blocked or covered by the protein deposit. Ho and Zydney (33) also developed a simpler analytical solution by assuming a spatially uniform cake

resistance, with results in good agreement with the detailed numerical calculations. Subsequent studies have extended this basic model framework to account for the effects of the membrane structure (34) and the underlying pore connectivity (35).

Ye et al. (27) analyzed the flux decline data during dead end unstirred filtration of sodium alginate (a model polysaccharide) using both the classical fouling models and the combined pore blockage and cake filtration model. The cake filtration model was able to effectively describe the flux decline data obtained with ultrafiltration membranes, but the combined pore blockage and cake filtration model was needed to analyze the experimental results obtained with 0.2 μm track-etched and 0.22 μm PVDF microfiltration membranes. Taniguchi et al. (29) examined the fouling behavior of ultrafiltration membranes during filtration of natural organic matter (NOM) isolated from a potable surface water. In this case the flux decline for the fresh (unfiltered) feed was well described using the cake filtration model. In contrast, the fouling was due primarily to pore blockage after prefiltration of the water to remove large aggregates. The combined pore blockage and cake filtration model was able to describe the data for both cases, including the observed change in fouling mechanism during the filtration experiment. Kilduff et al. (30) have used the combined pore blockage–cake filtration model to analyze flux decline data and evaluate the underlying fouling mechanisms for filtration of natural organic matter through a series of surface modified polyethersulfone membranes.

Figure 2 shows typical data for the filtrate flux as a function of time for the filtration of 0.25, 1, 2, and 4 mg/l humic acid solutions at a constant pressure

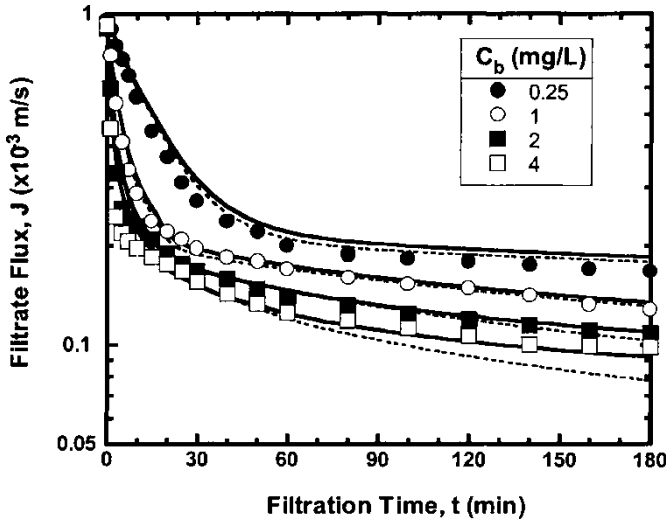

Figure 2. Flux decline behavior for filtraion of humic acid solutions. Taken from Yuan et al. (31).

of 35 kPa (5 psi) and a stirring speed of 300 rpm. The dashed curves in Fig. 2 represent model calculations using the combined pore blockage and cake filtration model (Eqs. (10) and (11)) with a single set of best fit parameters: α, $f'R'$, and R_{p0} (31). The model calculations are in very good agreement with the filtrate flux data over the entire filtration for the full range of humic acid concentrations using this single set of parameters. The model does tend to underpredict the flux for the 4 mg/L solution at long filtration times, which is probably related to the back transport of humic acids away from the membrane as discussed by Yuan et al. (31).

BACK TRANSPORT PHENOMENA

The rate of particle deposition on the membrane surface is reduced when there is intermolecular repulsion between the foulant and the membrane or additional hydrodynamic forces acting on the foulants. The hydrodynamic forces can include both inertial lift and shear induced diffusion. Shear induced diffusion occurs because of particle-particle collisions in the shear flow of a concentrated suspension (21, 36). Inertial lift arises from inertial interactions between particles and the flow boundary. Foulants can only deposit on the membrane surface when the drag force and other attractive interactions are able to overcome the hydrodynamic and repulsive forces that transport the particle back into the bulk suspension.

The back-transport phenomena can be included in the classical fouling models by re-writing the appropriate rate equation (equations (2), (5), and (8)) with an additional term to account for the removal of particles from the membrane. For example, the rate of cake growth in the cake filtration model would become:

$$\frac{dR_p}{dt} = f'R'(J - J^*)C_b \tag{12}$$

where J^* is the flux at which the rate of convective deposition is exactly balanced by the rate of back-transport. According to Eq. (12), the cake will continue to grow, and thus the flux will continue to decline, until a quasi-steady state is obtained with $J = J^*$. The solid curves in Figure 2 are model calculations using the combined pore blockage and cake filtration model accounting for back transport using equation (12).

Theoretical expressions for the steady-state flux have been derived for a number of different back-transport mechanisms. The steady-state flux for hydrodynamic models based on shear-induced diffusion and inertial lift can be expressed as a power law in the cross-flow velocity or shear rate (γ):

$$J^* = k \cdot \gamma^n \tag{13}$$

where n = 1 for shear-induced diffusion (21) and n = 2 for inertial lift (37). The steady-state flux also increases with increasing particle radius (a), with

a dependence on a^3 for inertial lift and $a^{1.33}$ for shear-induced diffusion. Thus, large cells and flocculated material tend to be kept away from the membrane, with the steady-state flux dominated by the smaller colloidal material.

A number of investigators have developed empirical correlations for the steady-state flux in terms of the wastewater properties and device operating conditions. For example, Shimizu (38) developed a correlation for the steady-state flux in terms of the superficial air velocity and the mixed liquor suspended solids concentration, while Krauth and Staab (39) included terms involving the Reynolds number and the difference between the mixed liquor suspended solids concentration and the mixed liquor volatile suspended solids concentration. These correlations can provide useful insights into some of the factors controlling the flux in MBR applications, but the specific functional form and fitted parameters are likely to be unique to the membrane, module design, wastewater, and biological status of the activated sludge.

Critical Flux

The critical flux is typically defined as the permeate flux below which there is little or no fouling since the rate of back transport is sufficient to eliminate particle deposition on the membrane. Operation at filtration velocities above the critical flux typically results in a rapid pressure rise during constant flux filtration or in a rapid flux decline during constant pressure operation. The critical flux can be evaluated experimentally by performing experiments using a pressure "stair-case" with the flux evaluated as a function of time at each constant pressure level along the stair-case. The critical flux is determined as the value of the flux below which the operation remains stable. A flux "stair-case" can also be used, with the transmembrane pressure measured as a function of time at each value of the flux. The critical flux is typically less than J^* since the quasi-steady flux for a given set of process conditions usually corresponds to a situation in which fouling has occurred and reached an equilibrium state.

Membrane bioreactors are generally operated below the critical flux in order to minimize fouling and obtain stable operation over relatively long periods of time. A number of strategies have been developed to increase the critical flux including air sparging (40–42), back flushing (43), addition of a flocculating agent, and/or increasing the cross-flow velocity (44). Gas sparging, back-flushing, and high cross-flow velocities disrupt the concentration polarization layer, facilitating the removal of the deposited cake layer. Backflushing is typically carried out periodically with back pulses of short duration (on the order of 0.1 s). The rate of back transport can also be increased through the use of fluid instabilities (45) generated by rough surfaces (46), turbulence promoters (47), or flow in highly curved channels (48, 49).

Gas sparging or bubbling is the most common approach for reducing fouling in membrane bioreactor systems since the air also provides oxygen for the biological treatment. In submerged hollow fiber systems, the air bubbles increase the local shear at the membrane surface, facilitating the removal of any deposited cake. Wicaksana et al. (50) have demonstrated that the bubbles also induce lateral fiber movement which can limit particle and cell deposition. The critical flux for a model hollow fiber unit used with Baker's yeast was greatest for fibers with small diameter, longer length, and loose packing, conditions that tend to enhance the lateral fiber movement.

Although the original development of the critical flux hypothesis was based on the assumption that there is no fouling below the critical flux, several recent studies have shown that a low level of fouling can take place even below the critical flux (51, 52). Sub-critical flux fouling typically occurs for complex feed streams containing soluble microbial products, extracellular polymeric substances, or cell lysates (53–56). Fouling under these conditions may be due to the heterogeneous distribution in the local flux over the surface of the membrane, with the high local flowrate through certain regions of the membrane (51) resulting in local fluxes that exceed the critical flux (57). Alternatively, fouling may be associated with the gradual evolution of the biomass over time, with the generation of more highly fouling species occurring in response to changes in the feed and/or the development of certain slow-growing microorganisms.

MEMBRANE MATERIALS

Microfiltration and ultrafiltration membranes for MBR can be made from a wide variety of materials, including different polymers (e.g., polyethersulfone, polyethylene, polypropylene, polytetrafluoroethylene, polyvinylidene fluoride, nylon, polyester, polycarbonate, cellulose acetate, and regenerated cellulose), ceramics (aluminum and zirconium oxide), glasses (borosilicate glass fiber), and metals (silver and stainless steel). Hydrophobic materials such as polyethersulfone and polyvinylidene fluoride (PVDF) are typically modified using proprietary surface treatments to render them more hydrophilic while the cellulosic, aluminum oxide, and polyester membranes are naturally hydrophilic. Although ceramic membranes have been examined for MBR applications (58, 59), the polymeric membranes dominate this market due to their lower cost and their availability as flexible hollow fibers. Fiber flexibility is particularly important in submerged MBR systems where fiber movement due to aeration can significantly improve the overall performance.

Several studies have demonstrated that membrane fouling is typically reduced for more hydrophilic surfaces. For example, Yu et al. (25) examined the behavior of a series of surface modified polypropylene membranes produced using a CO_2-plasma with different exposure times. Data were obtained in a single membrane bioreactor filled with activated

sludge obtained from a commercial wastewater treatment plant. The filtrate flux increased slightly with increasing plasma treatment, with a much greater effect seen in the flux recovery after washing with water, indicating that the more hydrophilic surfaces inhibited particle and biofilm adhesion. Similar results were obtained by Sainbayar (60) for polypropylene membranes modified by ozone treatment followed by graft polymerization with 2-hydroxy-ethyl methacrylate.

Membrane Morphology

In addition to the hydrophilicity, the surface roughness and pore morphology can both influence the fouling behavior. Kilduff et al. (61) analyzed fouling data for the filtration of natural organic matter through a series of polyethersulfone membranes with different surface roughness produced by UV irradiation followed by graft polymerization with N-vinyl-2-pyrrolidone. The rate of pore blockage, determined by fitting the filtrate flux data to equations (10) and (11), was greatest for the membrane that had been irradiated for the longest period of time, which the authors attributed to the increase in surface roughness.

Most polymeric microfiltration membranes consist of an isotropic network of polymer fibers resulting in a highly interconnected pore structure. The interconnected pore morphology for polyvinylidene fluoride (PVDF), cellulose acetate (CA), mixed cellulose ester (MF), and polytetrafluoroethylene (PTFE) membranes are shown in Fig. 3. The isotropic PVDF, CA, and MF membranes are formed by casting of the polymer in a solvent/non-solvent mixture, resulting in a network of polymer globules. The PTFE membranes are formed by controlled physical stretching of the polymer film followed by annealing at elevated temperature. The stretching process generates a structure with polymer nodules connected by thin fibers. These membranes tend to have a fairly broad pore size distribution throughout the membrane. Metallic membranes generally consist of an array of sintered metal particles or spheroids, giving an isotropic structure with more uniform pores in the interstices between the metal particles.

The polycarbonate (PCTE) and aluminum oxide (Anopore) membranes have structures with straight-through non-interconnected pores as shown in the scanning electron micrographs in Fig. 4. The PCTE membranes are made by the bombardment of a polycarbonate or polyester film with fission fragments followed by appropriate chemical etching. This yields a membrane with very uniform cylindrical pores (62). Pore density (porosity) can be controlled by irradiating the base polycarbonate for different periods of time. The pores in the Anopore membrane are formed from anodically oxidized aluminum and are somewhat more irregular in shape, although the pore size distribution is still quite narrow (63).

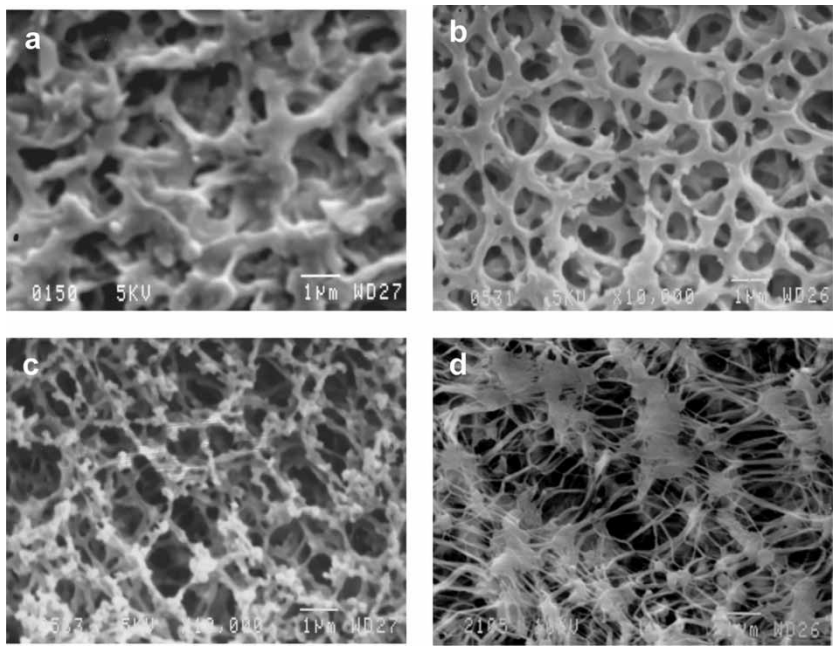

Figure 3. Scanning electron micrographs of the surface of (a) polyvinylidene fluoride (PVDF), (b) cellulose acetate (CA), (c) mixed cellulose ester (MF), and (d) polytetrafluoroethylene (PTFE) membranes.

Ho and Zydney (64) have demonstrated that the membrane morphology can have a significant effect on the rate of flux decline during protein filtration. Surface/pore blockage of membranes with straight-through (non-interconnected) pores causes a rapid decline in filtrate flux since the pore blockage completely eliminates fluid flow through the blocked pores

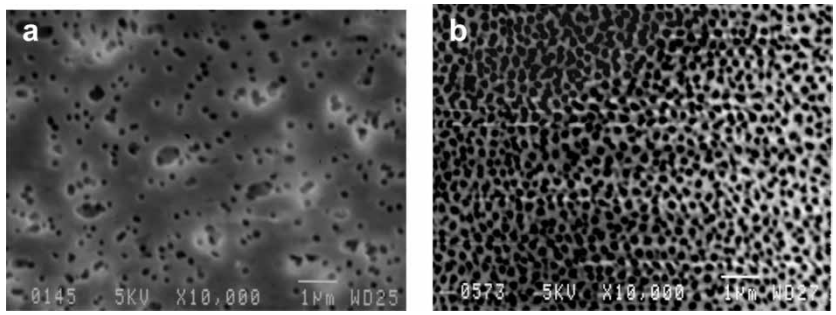

Figure 4. Scanning electron micrographs of the surface of (a) polycarbonate (PCTE) and (b) Anopore aluminum oxide membranes.

(upper panel of Fig. 5). In contrast, surface blockage of membranes with a highly interconnected pore structure causes relatively little decline in the filtrate flux since the fluid is able to flow under and around the blockage (right panel). Zydney and Ho (65) showed that the capacity of a polyvinylidene fluoride membrane having a highly interconnected pore structure is as much as four times larger than that of an Anopore membrane during protein microfiltration even though the membranes have very similar porosity, pore size, and initial permeability. Fratila-Apachitei et al. (66) showed a similar improvement in flux for ultrafiltration membranes having highly interconnected pore structures during the filtration of refinery and petrochemical wastewaters.

The fouling characteristics of isotropic membranes with different pore morphologies can be directly related to the extent of pore interconnectivity, defined as the ratio of the permeabilities in the lateral and normal flow directions through the membrane (64). Ho and Zydney (67) developed a novel experimental approach to evaluate this permeability ratio based on the relative fluid flow rate through a membrane that is partially covered with an impermeable tape. Membranes with very high degrees of interconnectivity show lower rates of flux decline due to the lateral flow around any blockage on the surface or within the porous depth of the membrane.

The flux decline behavior for composite and asymmetric membrane structures shows a more complex behavior (34). Surface fouling on these membranes completely blocks the pores in the upper skin layer, but the fluid rapidly re-distributes itself through the very highly interconnected pores within the membrane substructure. This causes a shunting of the

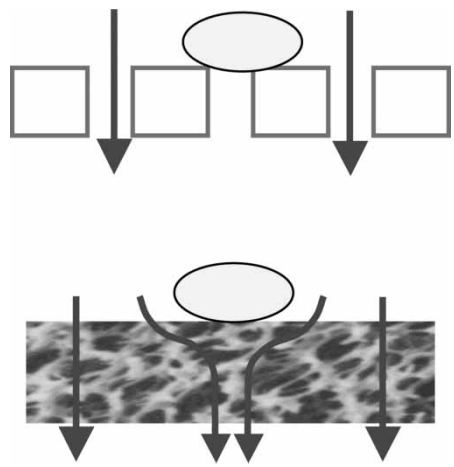

Figure 5. Schematic diagram showing the effects of the pore connectivity on the filtrate flux for a membrane with straight through non-interconnected pores (top panel) and for a membrane with a highly interconnected pore structure (bottom panel).

fluid flow towards the remaining open pores, leading to a reduction in the rate of flux decline compared to that for a single membrane layer. Ho and Zydney (34) have extended the basic pore blockage–cake filtration fouling model to account for the effects of this type of composite structure on the filtrate flux.

SUMMARY

Membrane bioreactors are now a well-established technology for wastewater treatment, with a significant number of systems installed around the world with capacities in excess of $1000\,m^3$/day. The integration of the membrane separation with the biological treatment provides greater control of the biological milieu, facilitating the degradation of toxic components while providing a higher quality effluent stream that is free of microorganisms.

Membrane fouling remains a critical issue in the design and operation of membrane bioreactors. The highly complex nature of the feed, including the high solids concentration and the diversity and variability of the biological components, creates real problems in both understanding and controlling fouling in these systems. Recent studies have clearly demonstrated the critical importance of extracellular polymeric substances, both as direct foulants and as stabilizing agents for biofilm formation on the membrane. However, the exact composition and properties of the EPS can vary significantly with time in response to changes in the feed water and the continual evolution of the physiologic environment in the MBR, including both the specific microorganisms and their biological activity.

Recent work has begun to provide a more fundamental understanding of the critical factors governing fouling in MBR systems, including the role of the membrane material, module, and operating conditions. Fouling in submerged MBR can be significantly reduced by proper aeration of the module due to the increase in local shear rate at the membrane surface in combination with the enhanced fiber movement, both of which increase back transport and reduce fouling. Operation below the critical flux has been shown to provide relatively stable performance over fairly long periods of time, but "sub-critical flux" fouling still occurs. The use of more hydrophilic membranes, often generated by controlled surface modification of synthetic polymers, can reduce EPS adsorption and minimize sub-critical flux fouling. New fouling models that include the combined effects of pore blockage and cake formation and also account for the membrane pore structure and interconnectivity have provided an improved framework for interpreting flux decline data and for identifying the underlying fouling mechanisms. Continued advances in our understanding of the effects of the mixed liquor composition, the membrane material, and the module design and operating conditions on membrane fouling should provide further improvements in MBR performance.

NOMENCLATURE

A	area of membrane available for filtration, m^2
A_0	initial area of membrane available for filtration, m^2
C_b	bulk concentration of foulant, kg/m^3
f'	fractional amount of total protein that contributes to deposit growth
J	filtrate flux, m/s
J^*	back-transport flux, m/s
k	proportionality coefficient for back-transport, m/s^{1-n}
n	exponent in back-transport model
N	number of membrane pores
ΔP	transmembrane pressure, N/m^2
Q	volumetric filtrate flow rate, m^3/s
Q_0	initial volumetric filtrate flow rate, m^3/s
Q_{open}	volumetric filtrate flow rate through open pores, m^3/s
r_p	radius of pore, m
r_0	initial pore radius, m
R_m	resistance of the clean membrane, m^{-1}
R_p	resistance of the deposit, m^{-1}
R_{p0}	initial resistance of a deposit, m^{-1}
R'	specific resistance of foulant deposit, m/kg
t	filtration time, s
t_p	time at which cake begins to grow, s
V	total collected filtrate volume, m^3

Greek Letters

α_1	pore blockage parameter, m^2/kg
α_{pore}	pore constriction parameter, m^3/kg
γ	wall shear rate, s^{-1}
δ_m	membrane thickness, m
σ_0	osmotic reflection coefficient
μ	fluid viscosity, kg/m/s
$\Delta\pi$	osmotic pressure difference, N/m^2

REFERENCES

1. Matson, S.L. and Quinn, J.A. (1986) Membrane reactors in bioprocessing. *Ann. NY Acad. Sci.*, 469: 152–165.
2. Chick, W.L., Perna, J.J., Lauris, V. et al. (1977) An artificial pancreas utilizing living beta cells: Effects on glucose hemostasis in diabetic rats. *Science*, 197: 780–782.

3. Stephenson, T.J., Jefferson, B., and Brindle, K. (2000) *Membrane Bioreactors for Wastewater Treatment*; IWA Publishing: London.
4. Cicek, N. (2003) A review of membrane bioreactors and their potential application in the treatment of agricultural wastewater. *Can. Biosys. Eng.*, 45: 37.
5. Yokomizo, T. (1994) Ultrafiltration membrane technology for regeneration of building waste-water for reuse. *Desalination*, 98: 319–326.
6. Fan, Y.B., Wang, J.S., Jiang, Z.C., Chen, M.X., Xu, K., and Jia, Z.P. (2000) Treatment of a dyeing wastewater from a woolen mill using an a/o membrane bioreactor. *J. Environ. Sci.*, 12: 344.
7. Manem, J.A.S. (1996) Membrane bioreactors. In *Water Treatment Membrane Processes*; Mallevialle, J., Odendaal, P.E. and Wiesner, M.R. (eds.); McGraw-Hill: New York, 17.11–17.31.
8. Cicek, N., Macomber, J., Davel, J., Suidan, M.T., Audic, J., and Genestet, P. (2001) Effect of solids retention time on the performance and biological characteristics of a membrane bioreactor. *Water Sci. and Technol.*, 43: 43–50.
9. Cicek, N., Franco, J.P., Suidan, M.T., Urbain, V., and Manem, J. (1999) Characterization and comparison of a membrane bioreactor and a conventional activated-sludge system in the treatment of wastewater containing high-molecular-weight compounds. *Water Environ. Res.*, 71: 64–70.
10. Marrot, B., Barrios-Martinez, A., Moulin, P., and Roche, N. (2004) Industrial wastewater treatment in a membrane bioreactor: A review. *Environ. Prog.*, 23: 59–68.
11. Ghyoot, W. and Verstraete, W. (2000) Reduced sludge production in a two-stage membrane-assisted bioreactor. *Water Res.*, 34: 205–215.
12. Wingender, J.N., Neu, T.R., and Flemming, H.-C. (1999) *Microbial Extracellular Polymeric Substances: Characterization, Structure, and Function*.
13. Dignac, M.F., Urbain, V., Rybacki, D., Bruchet, A., Snidaro, D., and Scribe, P. (1998) Chemical description of extracellular polymers: Implication on activated sludge floc structure. *Water Sci. and Technol.*, 38: 45–53.
14. Wisniewski, C. and Grasmick, A. (1998) Flee size distribution in a membrane bioreactor and consequences for membrane fouling. *Colloid Surface A*, 138: 403–411.
15. Defrance, L., Jaffrin, M.Y., Gupta, B., Paullier, P., and Geaugey, V. (2000) Contribution of various constituents of activated sludge to membrane bioreactor fouling. *Bioresource Technol.*, 73: 105–112.
16. Chang, I.S. and Lee, C.H. (1998) Membrane filtration characteristics in membrane-coupled activated sludge system—the effect of physiological states of activated sludge on membrane fouling. *Desalination*, 120: 221–233.
17. Nagaoka, H., Ueda, S., and Miya, A. (1996) Influence of bacterial extracellular polymers on the membrane separation activated sludge process. *Water Sci. and Technol.*, 34: 165–172.
18. Lesjean, B., Rosenberger, S., Laabs, C., Jekel, M., Gnirss, R., and Amy, G. (2005) Correlation between membrane fouling and soluble/colloidal organic substances in membrane bioreactors for municipal wastewater treatment. *Water Sci. and Technol.*, 51: 1–8.
19. Rosenberger, S., Evenblij, H., Poele, S.T., Wintgens, T., and Laabs, C. (2005) The importance of liquid phase analyses to understand fouling in membrane assisted activated sludge processes—six case studies of different European research groups. *J. Membrane Sci.*, 263: 113–126.
20. Hermia, J. (1982) Constant pressure blocking filtration laws—application to Power-Law Non-Newtonian fluids. *Trans. Inst. Chem. Eng.-Lond.*, 60: 183–187.

21. Zydney, A.L. and Colton, C.K. (1986) A concentration polarization model for the filtrate flux in cross-flow microfiltration of particulate suspensions. *Chem. Eng. Commun.*, 47: 1–21.
22. Meng, F.G., Zhang, H.M., Li, Y.S., Zhang, X.W., and Yang, F.L. (2005) Application of fractal permeation model to investigate membrane fouling in membrane bioreactor. *J. Membrane Sci.*, 262: 107–116.
23. Nuengjamnong, C., Kweon, J.H., Cho, J., Polprasert, C., and Ahn, K.H. (2005) Membrane fouling caused by extracellular polymeric substances during microfiltration processes. *Desalination*, 179: 117–124.
24. Zeman, L.J. and Zydney, A.L. (1996) *Microfiltration and Ultrafiltration: Principles and Applications*; Marcel Dekker: New York.
25. Yu, H.Y., Hu, M.X., Xu, Z.K., Wang, J.L., and Wang, S.Y. (2005) Surface modification of polypropylene microporous membranes to improve their antifouling property in MBR: NH3 plasma treatment. *Sep. Purif. Technol*, 45: 8–15.
26. Palacio, L., Ho, C.C., and Zydney, A.L. (2002) Application of a pore-blockage–Cake-filtration model to protein fouling during microfiltration. *Biotechnol. Bioeng*, 79: 260–270.
27. Ye, Y., Le Clech, P., Chen, V., Fane, A.G., and Jefferson, B. (2005) Fouling mechanisms of alginate solutions as model extracellular polymeric substances. *Desalination*, 175: 7–20.
28. Soffer, Y., Adin, A., and Gilron, J. (2004) Threshold flux in fouling of UF membranes by colloidal iron. *Desalination*, 161: 207–221.
29. Taniguchi, M., Kilduff, J.E., and Belfort, G. (2003) Modes of natural organic matter fouling during ultrafiltration. *Environ. Sci. Technol.*, 37: 1676–1683.
30. Kilduff, J.E., Mattaraj, S., Sensibaugh, J., Pieracci, J.P., Yuan, Y.X., and Belfort, G. (2002) Modeling flux decline during nanofiltration of NOM with poly(arylsulfone) membranes modified using UV-assisted graft polymerization. *Environ. Eng. Sci.*, 19: 477–495.
31. Yuan, W., Kocic, A., and Zydney, A.L. (2002) Analysis of humic acid fouling during microfiltration using a pore blockage-cake filtration model. *J. Membrane Sci.*, 198: 51–62.
32. Kosvintsev, S., Holdich, R.G., Cumming, I.W., and Starov, V.M. (2002) Modelling of dead-end microfiltration with pore blocking and cake formation. *J. Membrane Sci.*, 208: 181–192.
33. Ho, C.C. and Zydney, A.L. (2000) A combined pore blockage and cake filtration model for protein fouling during microfiltration. *J. Colloid Interface Sci.*, 232: 389–399.
34. Ho, C-C. and Zydney, A.L. (2001) Protein fouling of asymmetric and composite microfiltration membranes. *Ind. Eng. Chem. Res.*, 40: 1412–1421.
35. Zydney, A.L., Ho, C-C., and Yuan, W. (2003) Fouling phenomena during microfiltration: Effects of pore blockage, Cake filtration, and membrane morphology. In *New Insights into Membrane Science and Technology: Polymeric, Inorganic, and Biofunctional Membranes*; Bhattacharyya, D.B. and Butterfield, D.A. (eds.); Elsevier: Amsterdam, 27–44.
36. Eckstein, E.C., Bailey, P.G., and Shapiro, A.H. (1977) Self-diffusion of particles in shear flow of a suspension. *J. Fluid. Mech.*, 79: 191.
37. Belfort, G., Davis, R.H., and Zydney, A.L. (1994) The behavior of suspensions and macromolecular solutions in cross-flow microfiltration. *J. Membrane Sci.*, 96: 1–58.

38. Shimizu, K., Takada, S., Takahashi, T., and Kawase, Y. (2001) Phenomenological simulation model for gas hold-ups and volumetric mass transfer coefficients in external-loop airlift reactors. *Chem. Eng. J.*, 84: 599–603.
39. Krauth, K. and Staab, K.F. (1993) Pressurized bioreactor with membrane filtration for waste-water treatment. *Water Res.*, 27: 405–411.
40. Yu, K.C., Wen, X.H., Bu, Q.J., and Xia, H. (2003) Critical flux enhancements with air sparging in axial hollow fibers cross-flow microfiltration of biologically treated wastewater. *J. Membrane Sci.*, 224: 69–79.
41. Howell, J.A., Chua, H.C., and Arnot, T.C. (2004) In situ manipulation of critical flux in a submerged membrane bioreactor using variable aeration rates, and effects of membrane history. *J. Membrane Sci.*, 242: 13–19.
42. Psoch, C. and Schiewer, S. (2005) Long-term study of an intermittent air sparged MBR for synthetic wastewater treatment. *J. Membrane Sci.*, 260: 56–65.
43. Psoch, C. and Schiewer, S. (2005) Critical flux aspect of air sparging and back-flushing on membrane bioreactors. *Desalination*, 175: 61–71.
44. Madaeni, S.S., Fane, A.G., and Wiley, D.E. (1999) Factors influencing critical flux in membrane filtration of activated sludge. *J. Chem. Technol. Biot.*, 74: 539–543.
45. Winzeler, H.B. and Belfort, G. (1993) Enhanced performance for pressure-driven membrane processes—the argument for fluid instabilities. *J. Membrane Sci.*, 80: 35–47.
46. Jeffree, M.A., Peacock, J., Sobey, I.J., and Bellhouse, B.J. (1981) Gel layer limited hemofiltration rates can be increased by vortex mixing. *Clin. Exp. Dial. A.*, 5: 373–380.
47. Gupta, B.B., Howell, J.A., Wu, D., and Field, R.W. (1995) A helical baffle for cross-flow microfiltration. *J. Membrane Sci.*, 102: 31–42.
48. Mallubhotla, H., Hoffmann, S., Schmidt, M., Vente, J., and Belfort, G. (1998) Flux enhancement during Dean vortex tubular membrane nanofiltration 10. Design, construction, and system characterization. *J. Membrane Sci.*, 141: 183–195.
49. Chung, K.Y., Brewster, M.E., and Belfort, G. (1998) Dean vortices with wall flux in a curved channel membrane system: 3 Concentration polarization in a spiral reverse osmosis slit. *J. Chem. Eng. Jpn.*, 31: 683–693.
50. Wicaksana, F., Fan, A.G., and Chen, V. (2005) The relationship between critical flux and fibre movement induced by bubbling in a submerged hollow fibre system. *Water Sci. and Technol.*, 51: 115–122.
51. Ognier, S., Wisniewski, C., and Grasmick, A. (2004) Membrane bioreactor fouling in sub-critical filtration conditions: a local critical flux concept. *J. Membrane Sci.*, 229: 171–177.
52. Pollice, A., Brookes, A., Jefferson, B., and Judd, S. (2005) Sub-critical flux fouling in membrane bioreactors—a review of recent literature. *Desalination*, 174: 221–230.
53. Youravong, W., Lewis, M.J., and Grandison, A.S. (2003) Critical flux in ultrafiltration of skimmed milk. *Food Bioprod. Process.*, 81: 303–308.
54. Defrance, L. and Jaffrin, M.Y. (1999) Comparison between filtrations at fixed transmembrane pressure and fixed permeate flux: application to a membrane bioreactor used for wastewater treatment. *J. Membrane Sci.*, 152: 203–210.
55. Rosenberger, S. and Kraume, M. (2002) Filterability of activated sludge in membrane bioreactors. *Desalination*, 146: 373–379.
56. Mukai, T., Takimoto, K., Kohno, T., and Okada, M. (2000) Ultrafiltration behaviour of extracellular and metabolic products in activated sludge system with UF separation process. *Water Res.*, 34: 902–908.

57. Cho, B.D. and Fane, A.G. (2002) Fouling transients in nominally sub-critical flux operation of a membrane bioreactor. *J. Membrane Sci.*, 209: 391–403.
58. Cicek, N., Dionysiou, D., Suidan, M.T., Ginestet, P., and Audic, J.M. (1999) Performance deterioration and structural changes of a ceramic membrane bioreactor due to inorganic abrasion. *J. Membrane Sci.*, 163: 19–28.
59. Ahn, K.H., Song, J.H., and Cha, H.Y. (1998) Application of tubular ceramic membranes for reuse of wastewater from buildings. *Water Sci. Technol.*, 38: 373–382.
60. Sainbayar, A., Kim, J.S., Jung, W.J., Lee, Y.S., and Lee, C.H. (2001) Application of surface modified polypropylene membranes to an anaerobic membrane bioreactor. *Environ. Technol.*, 22: 1035–1042.
61. Kilduff, J.E. and Karanfil, T. (2002) Trichloroethylene adsorption by activated carbon preloaded with humic substances: Effects of solution chemistry. *Water Res.*, 36: 1685–1698.
62. Fleischer, R.L., Price, P.B., and Walker, R.M. (1963) Method of forming fine holes of near atomic dimensions. *Rev. Sci. Instrum.*, 34: 510.
63. O'Sullivan, J.P. and Wood, G.C. (1970) Morphology and mechanism of formation of porous anodic films on aluminium. *P. Roy. Soc. Lond. A. Mat.*, 317: 511.
64. Ho, C.C. and Zydney, A.L. (1999) Effect of membrane morphology on the initial rate of protein fouling during microfiltration. *J. Membrane Sci.*, 155: 261–275.
65. Zydney, A.L. and Ho, C-C. (2003) Effect of membrane morphology on system capacity during normal flow microfiltration. *Biotech. Bioeng*, 83 (5): 537–543.
66. Fratila-Apachitei, L.E., Kennedy, M.D., Linton, J.D., Blume, I., and Schippers, J.C. (2001) Influence of membrane morphology on the flux decline during dead-end ultrafiltration of refinery and petrochemical waste water. *J. Membrane Sci.*, 182: 151–159.
67. Ho, C.C. and Zydney, A.L. (2000) Measurement of membrane pore interconnectivity. *J. Membrane Sci.*, 170: 101–112.